Proceedings World Geothermal Congress 2020+1
Reykjavik, Iceland, April - October 2021

Development and Application of a Multiphase Reactive Transport Model for the Scaling of Geothermal System

Lihua Liu[1*], Dedong Li[2], Haizhen Zhai[1]

[1] Key Laboratory of Gas Hydrate, Guangzhou institute of energy conversion, Chinese academy of sciences, Guangzhou 510640, CHINA; [2] Institute of Geosciences, Christian-Albrechts-University Kiel, Kiel, Germany

liulh@ms.giec.ac.cn

Keywords: Multiphase flow, geochemical model, scaling of geothermal well, Yangbajing Tibet, simulation

ABSTRACT

A multiphase (gaseous, aqueous and solid phases) reactive transport model has been developed to simulate scaling process in the geothermal system. The model combines the Hagen-Poiseuille equation with a self-developed geochemical model. The equation describes the mass rate of flow, which could be annular or bubbly flow, and the mass conservation of a multiphase system in the round tube under varying temperature and pressure condition. The geochemical model quantitatively evaluates the vaporization and condensation process of aqueous fluid, and the dissolution and precipitation process of solid mineral and scale in the multiphase geothermal system. The numerical method and a computer program are used to obtain the numerical solution for the coupling model. Above simulation tool and numerical method could theoretically model the scaling process in a pipeline in a geothermal system. In this work, we investigate thermodynamic and geochemical process of scaling within a vertical well by using the conceptual simulation tool under the environmental condition of Yangbajing, Tibet. Yangbajing is a famous geothermal field for its abundant geothermal energy and also for its severely scaling. The results indicate that scaling initially appears under 100 m deep of the well, and the scaling layer will be 0.017 m thickness 24 hour after pumping. The couple simulation tool can be used for the design of the descaling/antiscalling system and technics, and the field data is needed for the improvement of the simulation tool.

1. INTRODUCTION

Geothermal is a kind of clean energy originates from the melting magma and radioactive decay of material and stores inside the earth. With the environmental hazard of fossil energy and controversy of nuclear power, the geothermal energy meets a new summit time of research and application. According to the The World Geothermal Congress 2015 Melbourne, Australia, more than 80 countries presented their technology and ventured on the geothermal energy. These countries included the United State, Japan, Iceland, Italy, New Zealand, Indian and Philippine etc. In China, the geothermal is mainly low or middle temperature energy and distributes around Tibet, Hebei, Guangdong, and petroleum producing area in the northern China. Recently, the application of geothermal energy in China dramatically increases, and the direct utilization has edged the top level of the world. Large area of hot dry rock has been explored in Gonghe, Qinghai Province. Xiong'an as an alternative center of capital has planned to set geothermal energy as main energy source. During the national thirteenth five-year plan, more geothermal energy related projects have been sponsored which will promote the research and technology of geothermal in China.

Geothermal energy, both shallow and deep has been used directly in heating supply, farming and bath in most part of China, or indirectly in power generating (Wang et al., 2000), which primarily utilizes in Tibet and Yunan Province. However, there are some restraints which impede the enhanced application of geothermal energy, and scaling is the one of these critical constrains. Almost all kind of application encounters the scaling, especially for the inside of the geothermal pipeline and valve. The operation cost will enormously jump if scale, utilization efficiency will decrease and may even clog the pipes and eventually discontinued the system.

The scale contains mainly sulfur metal, oxidized silica and carbonate, and also tiny amount of metal, aluminosilicates, clay minerals and sulfates (Alt-Epping et al., 2013; Diamond and Alt-Epping, 2014; Regenspurg et al., 2015). The compounds of scale, the initial time of scaling and precipitation rate in a certain well depends on the geological background and the design of application. The variation of compounds, scale time and precipitation rate cause the different of de-scale and the lifetime of the device (Liu, 2015). The scale in Tibet and eastern Sichuan area is mainly carbonate. The geothermal wells in Yanbajin area, Tibet have severely scaled since the first day of operation. Scale of deep geothermal system mainly contains silica and aluminosilicates (Diamond and Alt-Epping, 2014), the deposition rate generally slow compare to the shallow system. Once the 200 mm well was totally shut off after 5 days in Yangbajin (Ling et al., 1992). In Dangxiong, another area in Tibet, the solid phase had in 2008, deposited 30 mm within 15 days for a 300 mm supply pipe of geothermal spring (Xu, 2010). The 100 mm blowout line was choked within 8 days in Ganzi Kangding in 2014 (Wang et al., 2015).

Previously, a few researches in China focused on scaling. Wang etc. used Langelier and Ryzna saturation index to determine the probability of scale (Wang et al., 2015). Zhang et al. estimated the minerals deposited in one geothermal well in Ganzi area (Zhang et al., 2016). Several groups from Switzerland, the United States and Germany simulated the rock-fluid interaction at various depth of hot dry rock resource (Alt-Epping et al., 2013; Andre et al., 2006; Diamond and Alt-Epping, 2014; Fritz et al., 2010; Xu et al., 2004). However, we still have limit knowledge about the location, initial time and rate of deposition. We do not have the tool to estimate these factors which cause our mountain in labor to descale neither.

Currently, mechanical and chemical methods are generally adopted to descale (Ma and Tian, 2006). Mechanical method is just a simple way using a long iron rod to tamp down the scale deposit or pump the spring to a pool for deposition before further utilization. Chemical method generally change the pH or concentrations of ions with scale inhibitor to prevent the deposition (Xu et al., 2004). To decide the scheme of chemical descale, several trials are needed to choice the scale inhibitor and doze of the inhibitor. The trial needs manpower and materials and may also lead to unnecessary environmental problem.

This difficult situation motives this work. We thus developed a multiphase reactive transport model and would simulate the scaling of a geothermal system in a pipeline with the model. The results of the simulation could elucidate the mechanism of scale and reveals the scaling processes in detail. The model will be an assistant for the design of the descaling/antiscalling system and technics.

2. MULTIPHASE REACTIVE TRANSPORT MODEL UNDER VARIABLE TEMPERATURE AND PRESSURE

2.1 Schematic of the simulation tool

Geothermal system includes gaseous, aqueous and solid phase (minerals). The transport of the hot fluid combines reaction, diffusion, advection and phase transition under a variable temperature and pressure condition.

The gases, liquid and mineral coexist in the spring well. Gas is regarded as compressible and brine in the confine aquifer as incompressible. From the confine aquifer to the pipe and atmosphere, the location which is depth in the pipeline, temperature and pressure successively change, and phase suddenly changes including evaporation and deposition. Typical hydrological and heat transfer model could describe the successively changing of heat and fluid transport. And the evaporation and deposition however, could only be portrayed by geochemical model. The mineral generally deposit while the solubility product is higher than the equilibrium constant of a certain water-rock reaction. The evaporation is determined by the fugacity of the compound. The couple of deposition and evaporation with migration of fluid and heat is the critical point for the simulation. The difficult is the system being steady or equilibrium under a certain condition of temperature and pressure, the change of temperature and or pressure causes the composition and phase change, then phase change, in contrast affects the environmental temperature and pressure, these continuous changes form a interrelated system.

In this work, we will setup a model coupling above processes and effects. The schematic design of the coupling model is shown in Fig. 1.

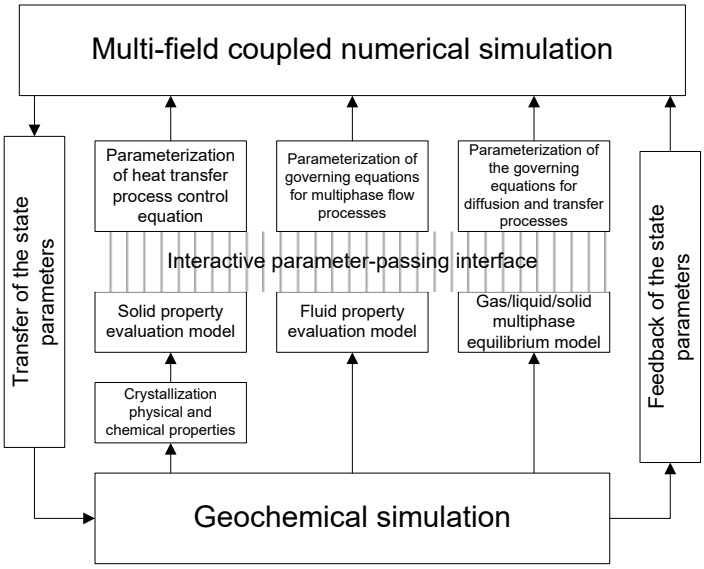

Figure 1: Schematic design and flowchart of the coupling model.

2.2 Setup of the fluid migration

The geothermal liquid was treated as an incompressible Newton liquid, the mass flow rate (*w,* in kg s^{-1}) describes the mass passing through a certain area within unit time. The flow rate is described by Hagen-Poiseuille equation as (Bird et al., 2002) (page 45):

$$w = \frac{\pi(\widehat{P}_0 - \widehat{P}_L) r^4 \rho}{8\mu L} \tag{1}$$

The very small amount of the liquid is treated as continuous quantity points and moving in free space. These quantities could be described as a continuous function of time and space.

$$\frac{\partial \rho}{\partial t} = -\frac{1}{S}\frac{\partial w}{\partial z} \tag{2}$$

where w is mass flow rate (kg s^{-1}), ρ is density (kg m^{-3}), μ is the visocity of liquid (Pa·s or kg $(s \cdot m)^{-1}$), L is the length of the tube (m), r is the diameter of the tube (m), $\widehat{P}$ is the modified pressure, $\widehat{P} = p + \rho g h$, h is the distance to the horizontal reference, generally takes the ground, $h = -z$ for the liquid in the confine zone, g is the normal acceleration of gravity (9.8m s^{-2}), S is the cross section area of the t (m^2), t is the time (s).

The Hagen-Poiseuille describes the fluid flow of *dz* pipeline, the approximate solution is (Bird et al., 2002) (page 161),

$$w = \frac{\pi r^4 \rho}{8 \mu f}\left(-\frac{\mathrm{d}p}{\mathrm{d}z} + \rho g\right) \tag{3}$$

where f is the apparent friction factor (-), a bulk non-ideal effect parameter describing the decrease of the flow rate by the pressure gradient.

Various methods could describe the multiphase fluid flow. Macroscopic model always treat the multiphase medium as continuous transport liquid and each phase could permeate to another phase. These kinds of models could be used in geothermal field. Microscopic model, in contract specially describes the movement inside a certain phase and or the interphase, could be used to depict the processes controlled by the interphase. The geothermal fluid passed through the tube, the flow includes annular and bubbly flow for both gaseous and aqueous phases. Micro-model of annular flow deals with the stratified, corrugated and circulating flow, the mass balance equation of annular flow could be (Oertel et al., 2008) (10.14, 10.15),

$$\frac{\partial}{\partial t}\left(\rho_{\mathrm{G}} \cdot \varepsilon \cdot S\right) + \frac{\partial}{\partial z}\left(\dot{m} \qquad S_{,} = \Gamma_{\mathrm{G}}\right. \tag{4}$$

$$\frac{\partial}{\partial t}\left[\rho_{\mathrm{L}} \cdot (1-\varepsilon) \cdot S\right] + \frac{\partial}{\partial z}\left[\dot{m} \qquad \cdot S\right] = \Gamma_{\mathrm{L}} \tag{5}$$

where subscript *G, L* indicates gaseous and liquid phase, $\dot{m}$ is the density of mass flux, Γ is the density of mass in the interphase, ε is the gas fraction.

Macro-model of dispersive flow describes the bubble flow, the mass balance equation is (Bird et al., 2002),

$$\frac{\partial \rho_{\mathrm{H}}}{\partial t} = -\frac{1}{S}\frac{\partial \dot{M}}{\partial z} \tag{6}$$

where subscript *H* indicates homogeneous, and $\rho_{\mathrm{H}} = \varepsilon \cdot \rho_{\mathrm{G}} + (1-\varepsilon) \cdot \rho_{\mathrm{L}}$, $\dot{M}$ is the total mass flux of all compounds.

$$\dot{M} \quad \llcorner \dot{M}_k \quad S \quad \llcorner \rho_k \varepsilon_k u_k \tag{7}$$

where subscript *k* here means gaseous or aqueous, *u* is the velocity of certain phase (m s^{-1}).

A tool combining above mass balance (Eqs. (4)(5) or (6)) to flow equation (Eq. (3)) and implementing the model, could be used to simulate the transport of compressive liquid inside the geothermal system. Further coupling to heat and phase transfer, the mode could then represent the scale in the geothermal system.

The heat conversion is,

$$\frac{\partial(\rho U)}{\partial t} + \nabla \cdot \left(\rho U v\right) + p\left(\nabla \cdot v\right) - \nabla \cdot \left(\lambda \nabla T\right) = 0 \tag{8}$$

The left part of the Eq. (8) is the change of internal energy over time, by compression and convection of the unit volume, respectively. Where, *t* is time (s), ρ is density (kg m^{-3}), *v* is the vector of speed (m s^{-1}), λ is the heat conductivity (J $(smK)^{-1}$), *T* is the temperature (K), *p* is the pressure (bar), *U* is the internal energy (kJ kg^{-1}), and the energy related to temperature as, $C_{\mathrm{V}} = \left(\frac{\partial U}{\partial T}\right)_{\mathrm{V}}$

The diffusion, advection and reaction of components in the system is,

$$\frac{\partial C_i}{\partial \mathrm{t}} + \nabla \cdot (C_i v) - \nabla \cdot (D_i \nabla C_i) - R_i = 0 \quad (i = 1,2,3 \ldots n) \tag{9}$$

The left part indicates rate of molar concentration increase with time, by advection, diffusion and reaction of *i* compound, respectively.

where *c* is molar concentration (mol m^{-3}), *D* is diffusion coefficient (m^2 s^{-1}), R_i is the reaction rate of *i* (mol m^{-3} s^{-1}) which is the critical part of scale and will be introduced in detail below.

2.3. Geochemical model

The geochemical system is controlled by several variables, temperature *T* (K), pressure *p* (bar) and composition *i*（*i*=1~n, in mol） as independent variable. Other variables need to be computed accordingly.

2.3.1 Phase state

Determination of the phase equilibrium parameters

Fugacity of the gas component *i* is,

$$f_i^V = y_i \phi_i p \tag{10}$$

Fugacity of liquid component *i* is,

$$f_i^L = x_i \gamma_i f_i \tag{11}$$

where f_i is the saturated pressure of *i* (bar), y_i and x_i is gas and liquid concentration of *i*-component in mol. ϕ_i and γ_i is fugacity and activity coefficient of *i* (-). Both fugacity and activity coefficient are functions of temperature, pressure and composition. For H_2O-CO_2 system equilibrium,

$$f_i^V = f_i^L \qquad i = \mathrm{H_2O, CO_2} \tag{12}$$

That is $y_i \phi_i p = x_i \gamma_i f_i$, the liquid molar fraction of CO_2, x_i is the saturated concentration of *i* (Duan and Sun, 2003). The gaseous concentration of H_2O is y_{H2O}, and,

$$y_{\mathrm{H_2O}} = x_{\mathrm{H_2O}} \gamma_{\mathrm{H_2O}} \phi_{\mathrm{H_2O}}^{sat} \left(p_{\mathrm{H_2O}}^{sat} / p \right) \cdot \left(PF_{\mathrm{H_2O}} / \phi_{\mathrm{H_2O}}^{V} \right) \tag{13}$$

where $\phi_{\mathrm{H_2O}}^{sat}$ is the fugacity coefficient of water (-), computed by state equation of water (Wagner and Kretzschmar, 2008), $PF_{\mathrm{H_2O}} / \phi_{\mathrm{H_2O}}^{V}$ is the function of temperature and pressure and the polynomial equation as (Duan and Li, 2008).

Determination of the density of aqueous and gaseous phase

The gas density is calculated by a cubic state equation while the system reaches equilibrium, here use Redlich-Kwong equation (Spycher and Pruess, 2010).

$$p = \left(\frac{RT}{V - b_{\mathrm{mix}}} \right) \cdot \left(\frac{a_{\mathrm{mix}}}{T^{1/2} V (V + b_{\mathrm{mix}})} \right) \tag{14}$$

where *V* is the molar volume (L mol^{-1}), *p* is pressure (bar), *T* is temperature (K), *R* is the gas constant (8.314J $(mol\ K)^{-1}$), a_{mix} and b_{mix} are interaction parameters of the system (compounds) (Spycher and Pruess, 2010)。

The molar volume of water containing CO_2 obtained according to (Li et al., 2011),

$$V = V_{\mathrm{B}} x_{\mathrm{B}} + V_{\varphi,\mathrm{CO_2}} x_{\mathrm{CO_2}} \tag{15}$$

where *B* is the brine molar volume (L mol^{-1}), $V_{\varphi,\mathrm{CO_2}}$ is CO_2 apparent partial molar volume (L mol^{-1}), that is the volume change due to the dissolution of CO_2, X_B, X_{CO2} is molar fraction of brine and CO_2.

2.3.1 Water-rock reaction

The equilibrium constant of water-rock reaction is defined according to the mass action law,

$$K_j = \prod_{i=1}^{N} \left(c_i \cdot \gamma_i \right)^{v_{ji}} \qquad j = 1 \sim N \tag{16}$$

The system is equilibrium while all reactions ($j = 1 \sim N$) reach equilibrium with the constants of K. The composition changing, the concentration and activity coefficient of compounds will also change, the equilibrium condition changes as well.

$$C = \left[c_1, c_2 \ldots c_N \right] \tag{17}$$

$$\Gamma = \left[\gamma_1, \gamma_2 \ldots \gamma_{N_s} \right] \tag{18}$$

where C_i indexes a matrix of concentration meeting the condition of Eq. (16). Meanwhile this matrix of concentrations determine the appropriated activity coefficients Γ in Eq. (18) and Eq. (16). While one concentration changed, the system became

disequilibrium and reacted further, until re-equilibrium with new matrix of concentrations (Eq. (16)). In addition, the variation of temperature and pressure leads to the shift of equilibrium constants *K*.

3. SIMULATE SCALING PROCESS IN YANGBJING, TIBET

Yangbajing is famous for its great amount of geothermal resource and also for its serious scaling (Duo, 2003; Duo and Ping, 2000; He, 1983; Jiang, 2009; Ling et al., 1992; Liu, 2015; Shen, 1985; Sun et al., 2015; Xi et al., 2013; Yang and Xin; Yin et al., 2016; Zhao et al., 1998a; Zhao et al., 1998b). We thus setup a model according to the reported data from Yangbajing and study the thermodynamic and chemical mechanism of scaling.

3.1 Model setup

The ground surface is the zero layer and increase down core till the bottom of the well, the length is 1000 m. An even grid was used and set 100 elements, with 101 nodes. The minerals in the bedrock are mainly quartz, aluminosilicates and tiny amount of carbonates. The ground thermal water is carbonate and CO_2 saturated, the CO_2 concentration is the solubility of the CO_2 under environmental condition (Duan and Sun, 2003). The parameters used in the model are listed in Table 1.

Table 1: Parameters of the model design.

Parameter	Unit	Value
Depth	m	1000
Grid	m	100
Radius	m	0.4
Surface temperature	K	473
Bottom temperature	K	553
Surface pressure	Bar	208
Bottom pressure	Bar	270
Salinity	g L^{-1}	2.8
Viscosity of gas	Pa.s	3.5×10^{-6}
Viscosity of liquid	Pa.s	5.5×10^{-4}

A self-developed code by C was adopted to compute above reaction equilibrium system with the input parameters of Table 1. The new concentration will obtain while the deviation is smaller than a defined accuracy (10^{-4}) and the program ends.

3.2 Simulation results

3.2.1 The state of the fluids under the field conditions

The simulation results display the state of the fluids under the field conditions in Figure 2 and 3.

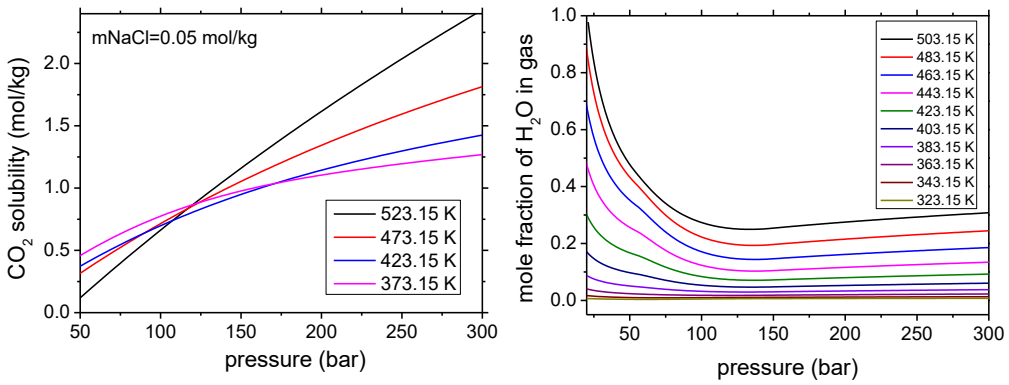

Figure 2: Solubility of CO_2 and mole fraction of H_2O under various pressure and temperature conditions.

The CO_2 solubility increases with the pressure under a certain temperature, in the high temperature area (473.15-523.15 K, by red and black lines), the temperature increases faster than the low temperature by blue and pink lines. While the gas containing mainly CO_2, the aqueous phase increases with the pressure decreases while the system pressure below 100 bar, and keeps almost constant while pressure is higher than 100 bar. The aqueous phase obviously increases with the temperature.

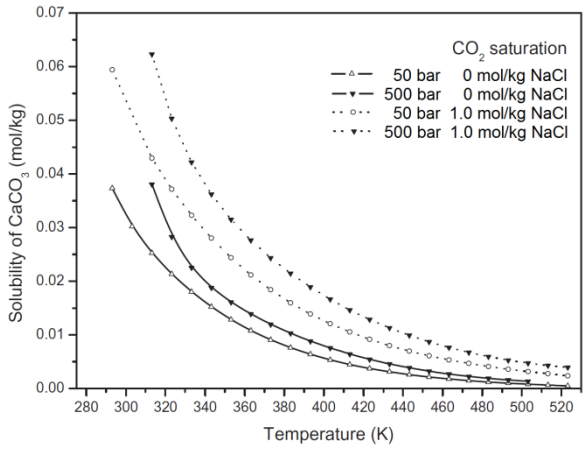

Figure 3: Solubility of $CaCO_3$ vs. temperature under various salinity and pressure conditions.

The solubility of carbonates vs. temperature under variable pressure and salinity is shown in Figure 3. If the aqueous solution containing with the dissolved CO_2, the carbonate drops with the temperature rises, the changing tendency is sharp during the range of 300-400 K, and steady for >400 K. This tendency is due to the acidity of carbonic acid falls with the temperature which causes the decrease of solubility. Figure 3 also indicates the solubility will dramatically climb with the salinity.

Solubility of CO_2 and $CaCO_3$ vs. pressure under various temperatures is shown in Figure 4. Under working range of geothermal well, the temperature (X axis) more obviously affects the carbonate solubility than pressure (Y axis). Even the CO_2 solubility (green dish line) is high under high temperature condition. The carbonate solubility is much lower from 423.15 to 373.15 K. The solubility of CO_2 crosses for the lines of 373.15 K and 423.15 K. The crossing is due to the effect of pressure to solubility being variable under different temperature. The solubility dramatically increase during high temperature zone (green dash line for 473.15 K), and steady for low temperature zone (red dash line for 373.15 K). Thus the solubility of high temperature could exceed the low one under high pressure condition, and form a cross of solubility line.

3.2.2 The physical fields inside the vertical well

The physical field and phase state of the fluid inside the well was also modelled. The pressure and density of fluids vs. depth inside the vertical well is demonstrated in Figure 5.

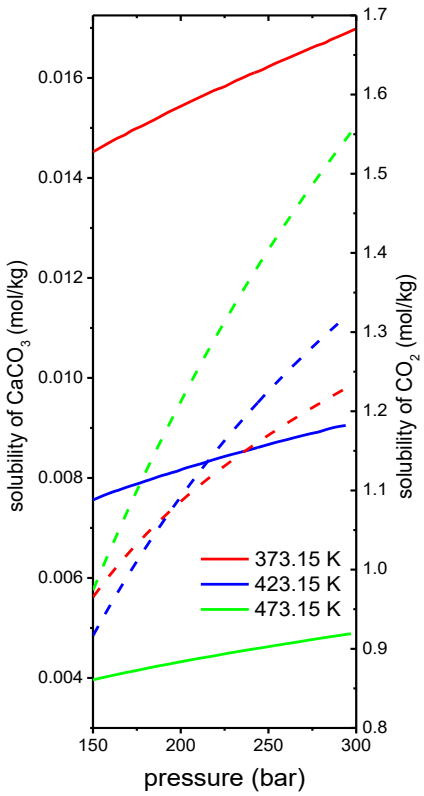

Figure 4: Solubility of CO_2 and $CaCO_3$ vs. pressure under various temperatures.

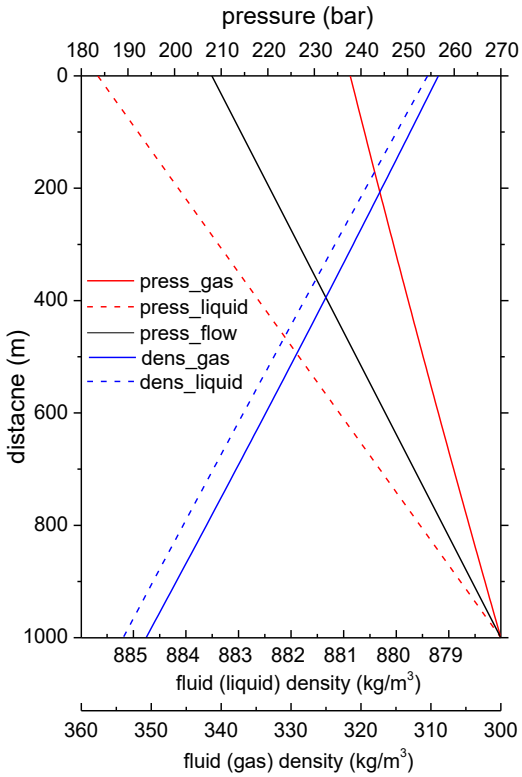

Figure 5: Pressure and density of fluids vs. depth.

The black solid line is the liquid pressure which is 270 bar at the bottom and linearly slips to 208 bar at the surface of the well (0 m depth). The red solid line shows the gas pressure if the liquid was only gas, which fixes 300 bar at 1000 m depth and the bottom is 238 bar. The gas pressure varies less than the well pressure due to the lighter density. Ant the red dash line shows the aqueous pressure if the fluid was only aqueous phase with a bottom pressure of 300 bar, the surface pressure becomes 184 bar. The difference is due to the density of liquid being heavy. We set the bottom (1000 m depth) pressure 270 bar for all phases, and the pressure changes rapidly for gas and slow for liquid.

The physical properties of the fluids inside the vertical well are shown in Figure 6. The fluids inside the well include gas and liquid (aqueous) phase. Black line is the gas saturation, and the density of mixture fluids (red line) lay on between gas (green line) and liquid (blue line). The density variation leads to the pressure variation.

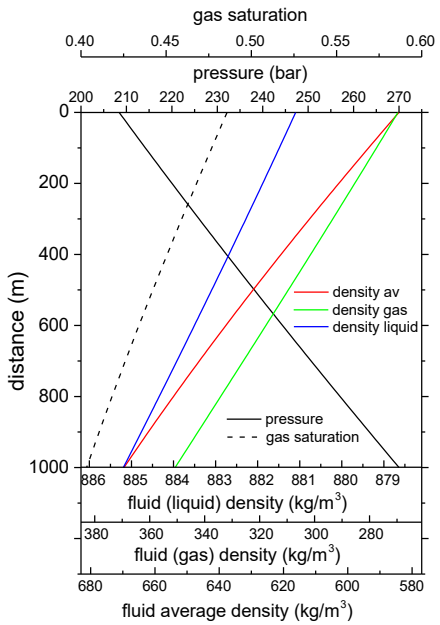

Figure 6: Physical properties of the fluids inside the vertical well.

The gas saturation and the volume of gas and liquid inside the vertical well is shown in Figure 7. The gas volume (black line) increases and liquid volume (red line) decreases from the surface to the bottom.

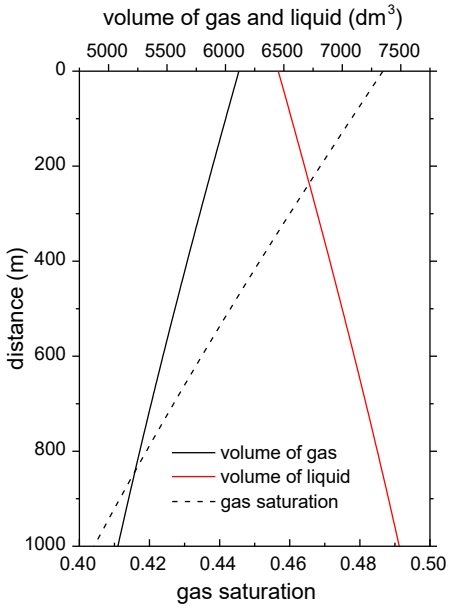

Figure 7: Gas saturation and the volume of gas and liquid inside the vertical well.

3.2.3 Coupling the geochemical and physical model

Formation of scale

The flow rate and composition of aqueous and gaseous phases could be estimated with the coupling of geochemical model and physical model. The scaling processes and thermodynamic mechanism could also be revealed.

The composition of aqueous and gaseous in the vertical well is shown in Figure 8. The aqueous contains 0.05 mol kg^{-1} NaCl. Carbonate is $CaCO_3$ with a saturated concentration (black dash line). Part of water is gas and marked as black line, thus the water content in aqueous phase (blue line) decreases. Ions of Na^+, Ca^{2+}, Cl^- could not enter into gas and only deposit as scale while water evaporates.

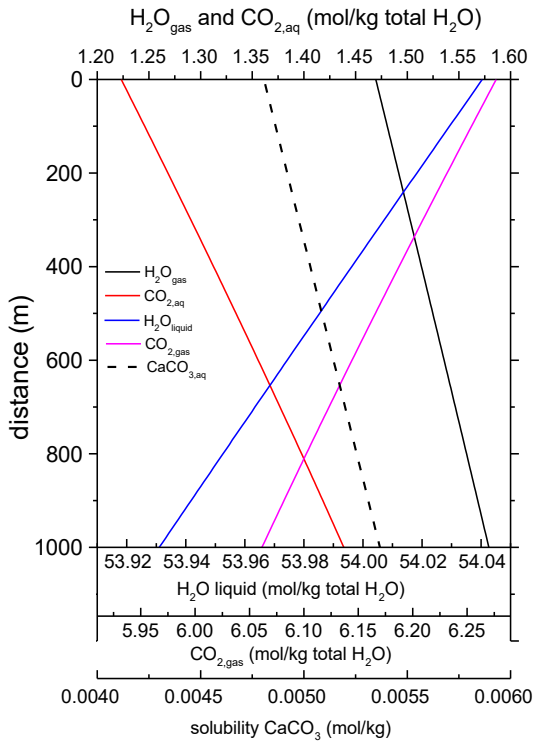

Figure 8: Components and fractions of the liquids inside the vertical well.

Comparison of the annular and bubble flow model

The simulation results are significant different with annual (Eqs. (4) or (5)) or bubble flow model (Eq. (6)). The comparison is shown in Table 2 and Figure 9.

Table 2. Simulation result of the circulation and bubbly flow.

	Unit	Annual flow	Bubble flow
Gas flow rate	kg s^{-1}	700	90
Liquid flow rate	kg s^{-1}	80	80
H_2O_gas	kg s^{-1}	61.25	7.875
CO_2_gas	kg s^{-1}	638.75	82.125
H_2O_aq	kg s^{-1}	75.4	75.4
CO_2_aq	kg s^{-1}	4.6	4.6
Deposition rate of $CaCO_3$	g s^{-1}	27	3.5
The depostion of inside well after 24 h, the density of scale is 2.7 kg L^{-3}			
Volume of $CaCO_3$	L	864	112
Volume of NaCl	L	25	3.25
Total volume (porosity 0.15)	L	1045.9	135.6
Thickness in the top of well	m	0.0166	0.0022
Radium of well	m	0.1834	0.1978

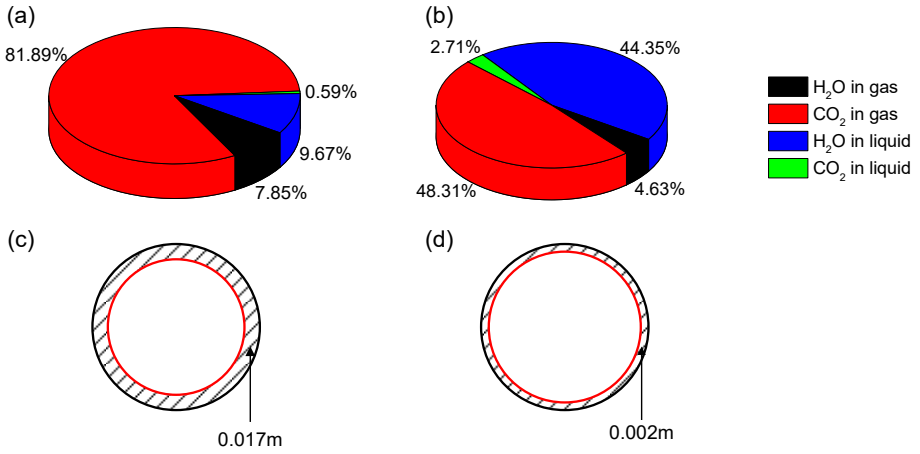

Figure 9: Component fraction of the outflow and the scaling inside the well 24 hours after pumping.

Table 2 shows that the gas volume flow rate and mass flow rate are higher than liquid due to its low viscosity. The ascending of water in gaseous phase causes by the evaporation and results in over saturation of $CaCO_3$. Scale initially presents in 100 m depth below the surface.

Figure 9a, the pie demonstrates the component fraction and outflow with an annual flow, and Figure 9b with the bubble flow. More gas will be produced under annual flow, and gas and aqueous is similar under bubble flow. The thickness of scale in the surface of the well is shown in Figure 9c and 9d for annual and bubble flow, respectively. Obviously, the annual flow with high gas flow rate will enhance the scaling process compare to bubble flow. The pressure goes down near the ground (Figure 5), and gas saturation goes up (Figure 7) which causes the evaporation and promotes the scale. The rough surface with scale will further affect the flow and may even block the pipe line.

4. CONCLUSION AND DISCUSSION

A multiphase reactive transport model has been developed in this work. Coupling the model with geochemical model could be used to theoretically simulate the phase change and formation of scale of the geothermal system. With this coupling model, the scaling processes and mechanism has been revealed based on the field date of Yangbjing, Tibet.

4.1 Critical condition of scaling process

The oversaturation of the geothermal fluid directly results in the scale. The precipitation of scale could be more serious if the flow rate and phase equilibrium dramatically changes which will also promote the geochemical reactions. Figure 4 shows the saturation of CO_2 obviously changes with the pressure variation and affects the pH of the solution. The saturation of carbonate keeps relatively constant with the variation of pressure, which totally excludes the pressure effect of scale there.

4.2 Thermodynamic and geochemical mechanism of scaling process

The typical high temperature geothermal fluids contain both gaseous and aqueous phases. The pressure of the system lies in between pure gas and water (Figure 6). The flow rate of gaseous phase is clearly higher than aqueous phase (Table 2). Thus the effluent contains a certain amount of gaseous H_2O even if the main fraction is still CO_2 (Figure 8). The gaseous H_2O cannot dissolve salt or aqueous species, thus enhances the formation of scale. The scaling becomes less serious when the flow is bubby and contains equivalent gas and water.

4.3 The simplification and lookout of the model

The coupling model excludes the effect of friction and slide. Some parameters, e.g. the porosity, flow type and relative flow rates of gas and water were all estimated rather than determination. The exclusion and estimation parameters definitely affect the precision of the model result. In conclusion the field data of the composition, concentration and flow rate are necessary for the further modify the model and evaluate the scaling and produce of the geothermal system.

ACKNOWLEDGEMENT

This work was financially supported by the NSF of China (Grant number: 417760711).

REFERENCES

Alt-Epping, P., Waber, H. N., Diamond, L. W., and Eichinger, L., Reactive transport modeling of the geothermal system at Bad Blumau, Austria: Implications of the combined extraction of heat and CO2: *Geothermics*, 2013, v. **45**, p. 18-30.

Andre, L., Rabemanana, V., and Vuataz, F. D., Influence of water-rock interactions on fracture permeability of the deep reservoir at Soultz-sous-Forets, France: *Geothermics*, 2006, v. **35**, no. 5-6, p. 507-531.

Bird, R. B., Stewart, W. E., and Lightfoot, E. N., Transport Phenomena, Beijing, Chemical Industry Press. 2002,

Diamond, L. W., and Alt-Epping, P., Predictive modelling of mineral scaling, corrosion and the performance of solute geothermometers in a granitoid-hosted, enhanced geothermal system: *Applied Geochemistry*, 2014, v. **51**, p. 216-228.

Duan, Z., and Li, D., Coupled phase and aqueous species equilibrium of the H2O–CO2–NaCl–CaCO3 system from 0 to 250°C, 1 to 1000bar with NaCl concentrations up to saturation of halite: *Geochimica et Cosmochimica Acta*, 2008, v. **72**, no. 20, p. 5128-5145.

Duan, Z., and Sun, R., An improved model calculating CO2 solubility in pure water and aqueous NaCl solutions from 273 to 533 K and from 0 to 2000 bar: *Chemical Geology*, 2003,v. **193**, no. 3, p. 257-271.

Duo, J., The Basic Characteristics of the Yangbajing Geothermal Field —A Typical High Temperature Geothermal System: *Engineering Science*, 2003, v. **5**, no. 1, p. 42-47.

Duo, J., and Ping, Z., Characteristics and genesis of the Yan bajing geothermal field, Tiebet, in *Proceedings* Worlk Geothermal Congress, Kyshu-Tohoku, Japan, 2000, p. 1083-1088.

Fritz, B., Jacquot, E., Jacquemont, B., Baldeyrou-Bailly, A., Rosener, M., and Vidal, O., Geochemical modelling of fluid-rock interactions in the context of the Soultz-sous-Forets geothermal system: *Comptes Rendus Geoscience*, 2010, v. **342**, no. 7-8, p. 653-667.

He, S., Hydrogeochemical characterization of Yangbajin geothermal field: *Geology in China*, 1983, v. **6**, p. 19-21.

Jiang, Y., anticorrosio research and application of the devices in the power plant of Yangbajing geothermal field, in *Proceedings* Geothermal workshop in the Western Pacific Branch of the International Geothermal Association, Chengdu, 2009.

Li, D., Graupner, B. J., and Bauer, S., A method for calculating the liquid density for the CO2–H2O–NaCl system under CO2 storage condition: Energy Procedia, 2011, v. **4**, no. 0, p. 3817-3824.

Ling, Y., Tang, L., and Liu, S., Chemical descaling technics of geothermal well, in *Proceedings* International Symposium on geothermal development and utilization of China's Tibet,1992, Geological Publishing House.

Liu, M., A Review on Controls of Corrosion and Scaling in Geothermal Fluids: *Advances in New and Renewable Energy*, 2015, v. **3**, no. 1, p. 38-46.

Ma, L., and Tian, S., The present situation of geothermal energy exploitation and utilization and its development trend in China: *Resource Industrial Economy*, 2006, v. **9**, p. 19-21.

Oertel, H., Prandtl, L., Boehle, M., and Mayes, K., Prandtl's Essentials of Fluid Mechanics, Beijing, Science Press. 2008,

Regenspurg, S., Feldbusch, E., Byrne, J., Deon, F., Driba, D. L., Henninges, J., Kappler, A., Naumann, R., Reinsch, T., and Schubert, C., Mineral precipitation during production of geothermal fluid from a Permian Rotliegend reservoir: *Geothermics*, 2015, v. **54**, p. 122-135.

Shen, X., The resources assessment of first geothermal field in China: Chinese Science Bulletin, 1985, v. **15**, p. 1171-1174.

Spycher, N., and Pruess, K., A Phase-Partitioning Model for CO2–Brine Mixtures at Elevated Temperatures and Pressures: Application to CO2-Enhanced Geothermal Systems: *Transport in Porous Media*, 2010, v. **82**, no. 1, p. 173-196.

Sun, H., Ma, F., Ling, W., Liu, Z., Wang, G., and Dawa, N., Geochemical characterization and utilization of thermometric scale of high temperature geothermal fields in Tibet: *Geological Science and Technology Information*, 2015, v. **34**, no. 3, p. 171-177.

Wagner, W., and Kretzschmar, H.-J., International Steam Tables - Properties of Water and Steam based on the Industrial Formulation IAPWS-IF97, 2008, Springer.

Wang, G., Zhang, F., and Liu, Z., An Analysis of Present Situation and Prospects of Geothermal Energy Development and Utilization in the World: *Acta Geologica Sinica*, 2000, v. **21**, no. 2, p. 134-139.

Wang, Y., Liu, S., Bian, q., Yan, B., Liu, X., Liu, J., Wang, H., and Bo, X., Scaling Analysis of Geothermal Well from Ganzi and Countermeasures for Anti-scale: *Advances in New and Renewable Energy*, 2015, v. **3**, no. 3, p. 202-206.

Xi, M., Ma, S., Zhu, L., and Li, B., Geochemical characteristics of dispersed elements in stream sediments of Yangbajin-Nyingzhong Area, Tibet and Their Significance in Ore prospecting: *Acta Geologica Sinica*, 2013, v. **34**, no. 6, p. 702-712.

Xu, T. F., Ontoy, Y., Molling, P., Spycher, N., Parini, M., and Pruess, K., Reactive transport modeling of injection well scaling and acidizing at Tiwi field, Philippines: *Geothermics*, 2004, v. **33**, no. 4, p. 477-491.

Xu, Y., Key Technolog of development and utilization of geothermal energy in Tibet - Solving the problem of scaling, in *Proceedings* Achievements and Prospect - Li Siguang promote the development and utilization of geothermal energy in China, the 40 anniversary conference and seminar on geothermal development in China, 2010, Geological Publishing House.

Yang, Q., and Xin, K., A brief introduction to the geothermal system of the Yangbajin Geothermal field: *Geological Review,* 1991, v. **37**, no. 3, p. 283-287.

Yin, M., Zhang, G., He, J., and Yan, F., Biological activity and diversity of moderately thermophilic actinomyccetes from geothermal field in Yangbajing of Tibet: *Journal of Anhui Agri. Sci.*, 2016, v. **44**, no. 12, p. 1-4.

Zhang, H., Hu, Y., Yun, Z., and Qu, Z., Applying Hydro-Geochemistry Simulating Technology to Study Scaling of the High-Temperature Geothermal Well in Kangding County: *Advances in New and Renewable Energy*, 2016, v. **4,** no. 2, p. 111-117.

Zhao, P., Ji, D., Liang, T., Jin, J., and Zhang, H., Chemical composition of gas of thermal water in the Yangbajing geothermal field, Tibet: *Chinese Science Bulletin*, 1998a, v. **43**, no. 7, p. 691-696.

Zhao, P., Jin, J., Zhang, H., Ji, D., and Liang, T., Chemical composition of thermal water in the Yangbajing geothermal field, Tibet: *Scientia Geologica Sinica*, 1998b,v. **33**, no. 1, p. 61-72.